

# Numerical approaches to solving a nonlinear system of Schrödinger equations for wave propagation in an optical fiber

A. J. SAKHABUTDINOV, V. I. ANFINOGENTOV, O. G. MOROZOV, R. R. GUBAIDULLIN  
Kazan National Research Technical University n. a. A.N. Tupolev — KAI, 420111, Kazan, Russia  
Corresponding author: Sakhabutdinov Airat J., e-mail: [azhsakhabutdinov@kai.ru](mailto:azhsakhabutdinov@kai.ru)

*Received September 4, 2019, revised January 13, 2020, accepted January 30, 2020*

The paper discusses approaches to the numerical integration of the second-kind Manakov equation system. Emphasis is placed on the transition from writing equations in dimensional quantities to equations in dimensionless units. A combined explicit/implicit finite-difference integration scheme based on the implicit Crank — Nicolson finite-difference scheme is proposed and substantiated, which allows integrating a nonlinear system of equations with a choice of nonlinear term at the previous integration step. An algorithm for levelling the disadvantage associated with the definition of the nonlinear term from the previous integration step is proposed. The approach of automatic selection of the integration step, which reduces the total number of integration steps while maintaining the required accuracy of the approximate solution, is substantiated. Examples of the calculation results for some values of the disturbance propagation are given. The limitations imposed by the computing scheme on the length of the integrable fiber section are described, and approaches, that eliminate these limitations without the need to increase arrays dimensions, are proposed. Requirements for initial boundary conditions are discussed.

*Keywords:* Manakov equation system, implicit/explicit Crank — Nicolson scheme, wave propagation, Schrödinger equations, optical fiber.

*Citation:* Sakhabutdinov A.J., Anfinogentov V.I., Morozov O.G., Gubaidullin R.R. Numerical approaches to solving a nonlinear system of Schrödinger equations for wave propagation in an optical fiber. Computational Technologies. 2020; 25(2):80–91.

## Introduction

Due to the presence of wave properties in microparticles, classical mechanics cannot give a correct description of their behavior. However, this can be done with the help of quantum mechanics created by Schrödinger, Heisenberg, Dirac, and others. The basic equation of quantum mechanics is the Schrödinger equation. The state of microparticles in quantum mechanics is described by the wave function, which is a function of coordinates and time and can be found by solving the Schrödinger equation, which relates the wave function to the particle mass, the Planck constant, and the potential energy of the particle in the force field in which it moves.

The Schrödinger equation, like Newton's equation in classical mechanics, cannot be obtained theoretically, since it is a generalization of a large number of experimental facts. The

validity of this relation is proved by the fact that all the consequences arising from it are consistent with the observed experimental facts and the empirical results.

The propagation of light in fiber optics is described by the nonlinear Schrödinger equation, where nonlinearity arises due to the Kerr effect. Nonlinearity is a problem for the transmission of information with the currently used modulation format in fiber-optic communication. Indeed, the greater the intensity, the more distorted the signal by nonlinear crosstalk, which limits the receiver's ability to recover the transmitted information. The task is to neutralize nonlinear effects in order to compensate for distortion and provide a high speed of information transmission through a nonlinear fiber optic channel. So far, two main ways of solving this problem have been undertaken: the first approach is to soften nonlinear effects using special methods, the second way is to specially encode information in the eigenmodes of the nonlinear channel. The second approach is based on integrating the nonlinear Schrödinger equation.

The description of the propagation of light, given its polarization dynamics, may, under certain conditions, which are applicable to modern fiber optic communication lines, be described by the Manakov equations, which are special case of the Schrödinger equations [1, 2].

## 1. Formulation of the problem

Suppose there are two polarizations with samples of complex signals in the time domain with some modulation (for example, 16QAM), which allows transmitting spectral efficiency. Physical signals propagate over fiber are continuous, but transmitted and received signals are considered discrete in time. After the signal propagates through the fiber, a signal with distributed nonlinearity and linear distortions due to chromatic dispersion can be obtained [3]. The fiber channel model can be represented using the system of nonlinear Manakov equations (1) [4, 5]:

$$\begin{cases} \frac{\partial E_1}{\partial \xi} = -i \frac{\beta_2}{2} \frac{\partial^2 E_1}{\partial \tau^2} + i\gamma \frac{8}{9} (|E_1|^2 + |E_2|^2) E_1 - \frac{\alpha}{2} E_1, \\ \frac{\partial E_2}{\partial \xi} = -i \frac{\beta_2}{2} \frac{\partial^2 E_2}{\partial \tau^2} + i\gamma \frac{8}{9} (|E_1|^2 + |E_2|^2) E_2 - \frac{\alpha}{2} E_2, \end{cases} \quad (1)$$

where  $E_1 = E_1(\xi, \tau)$  and  $E_2 = E_2(\xi, \tau)$ ,  $\xi$  — a spatial coordinate along a central axis of the optical fiber,  $\tau$  — time,  $E_1$  and  $E_2$  — polarizations, each of which is a complex function,  $i$  — the imaginary unit,  $\alpha$ ,  $\beta_2$ ,  $\gamma$  given process constants. Under given boundary conditions in the form:

$$\begin{aligned} E_1(L, \tau) = E_{01}(\tau), \quad E_1(\xi, 0) = E_1(\xi, T_0) = 0, \\ E_2(L, \tau) = E_{02}(\tau), \quad E_2(\xi, 0) = E_2(\xi, T_0) = 0, \end{aligned} \quad (2)$$

where  $L$  — the length of an optical fiber cable,  $T_0$  — the propagation time. The boundary conditions (2) at the end of  $L$  are specified as functions  $E_{01}(\tau)$  and  $E_{02}(\tau)$ , specified in discrete time samples as values of functions  $E_{01}(\tau_n)$  and  $E_{02}(\tau_n)$ , with  $\tau_n = \tau_0 + \Delta\tau n$ ,  $\Delta\tau = T_0/N$ ,  $n = \overline{0, N}$  [6].

The task is to find a solution for backscattering [7] in the form of dependencies (3):

$$E_1(0, \tau) \quad \text{and} \quad E_2(0, \tau), \quad (3)$$

which can also be determined at discrete points in time.

## 2. Equation system

The initial system of equations (1) in dimensional variables is inconvenient for its numerical solution. To move from problem statement in dimensional values to dimensionless values, it is necessary to replace variables (4):

$$x = \frac{E_1}{\sqrt{P}}, \quad y = \frac{E_2}{\sqrt{P}}, \quad t = \frac{\tau}{T_0}, \quad z = -\frac{\xi}{L}, \quad P = \frac{|\beta_2|}{(8/9)\gamma T_0^2}, \quad (4)$$

where  $L$  and  $T_0$  are related by  $L = 2T_0^2/|\beta_2|$ .

The system of equations in dimensionless quantities will be written as (5):

$$\begin{cases} i \frac{\partial x}{\partial z} = \frac{\partial^2 x}{\partial t^2} + 2\Phi(x, y)x, \\ i \frac{\partial y}{\partial z} = \frac{\partial^2 y}{\partial t^2} + 2\Phi(x, y)y, \end{cases} \quad (5)$$

where the nonlinear term is written in the form of the product of the desired function to the nonlinear part, for which the notation is introduced (6):

$$\Phi(x, y) = -i\alpha + |x|^2 + |y|^2. \quad (6)$$

The boundary conditions in this case will take the form:

$$\begin{aligned} x(-1, t) = x_0(t), \quad x(z, 0) = x(z, 1) = 0, \\ y(-1, t) = y_0(t), \quad y(z, 0) = y(z, 1) = 0. \end{aligned} \quad (7)$$

The formulation of the problem in terms of the initial conditions is initially given on a discrete set of points, it is logical and the solution would be to look numerically, writing the initial relations in a finite-difference form.

## 3. Difference scheme

The classical implicit difference scheme Crank—Nicolson (Fig. 1) was used to write equations (5) in the finite-difference form. The choice of the difference scheme is due to the fact that it is implicit, which makes it absolutely stable. Another advantage of the Crank—Nicolson scheme is that when integrating the equations of mathematical physics with the first derivative with respect to one and the second derivative with respect to another variable, it leads to the need to solve a system of linear equations with three diagonal matrices at each integration step, which is performed by a simple tridiagonal matrix algorithm [8].

In the Crank—Nicolson scheme, the coordinate grid is used in space and time, in the scheme in Fig. 1, the variable  $n$  is used to designate the layers in time, and the variable  $k$  in space. The parameters on the  $k+1$  layer of the coordinate grid are considered known, at the same time, the known values should be the initial and boundary values for  $k=K(z=-1)$ ,  $n=0(t=0)$ ,  $n=N(t=1)$ . In Fig. 1, the known values are indicated by gray circles, the values that need to be determined are the unfilled circles.

For the system of equations (5), the integration scheme, written in a completely implicit form, not only does not lead to the three-diagonal system of linear equations, but does not even lead to a linear system of equations. Let us write the system of equations (5) in

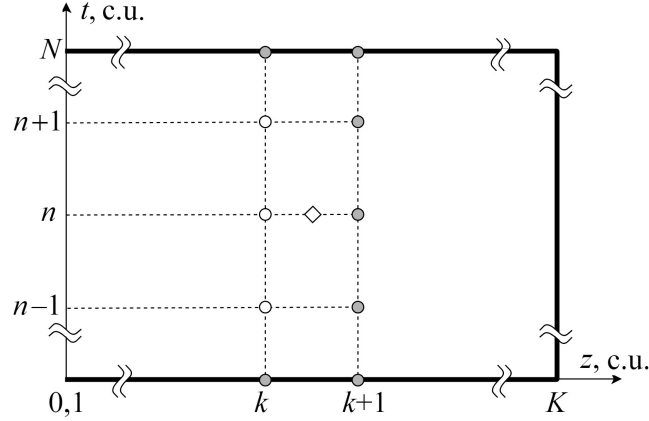


Fig. 1. The finite-difference scheme used to solve the system of equations: the rhombus in the figure indicates the point for which the equality of the system of equations is written; circles — nodes of a finite-difference scheme

the finite-difference form, using the six-point Crank — Nicolson scheme, having entered two parameters  $\sigma$  and  $\theta$ , changing in the range  $[0, 1]$ , the defining position of a shift for writing the finite-difference relations between the two (known and unknown) layers of integration.

The parameter  $\sigma$  is responsible for the implicit record of the linear part of equations (5), and the parameter  $\theta$  is separately allocated for the implicit record of a nonlinear multiplier  $\Phi(x, y)$ . The first derivative in space is written by first-order precision relations for a node  $(k + 1/2, n)$ .

$$\begin{cases} i \frac{(x_{k+1}^n - x_k^n)}{\Delta z} - \frac{\sigma(x_k^{n-1} - 2x_k^n + x_k^{n+1}) + (1 - \sigma)(x_{k+1}^{n-1} - 2x_{k+1}^n + x_{k+1}^{n+1})}{\Delta t^2} = \\ = 2(\theta\Phi_k^n + (1 - \theta)\Phi_{k+1}^n)(\sigma x_k^n + (1 - \sigma)x_{k+1}^n), \\ i \frac{(y_{k+1}^n - y_k^n)}{\Delta z} - \frac{\sigma(y_k^{n-1} - 2y_k^n + y_k^{n+1}) + (1 - \sigma)(y_{k+1}^{n-1} - 2y_{k+1}^n + y_{k+1}^{n+1})}{\Delta t^2} = \\ = 2(\theta\Phi_k^n + (1 - \theta)\Phi_{k+1}^n)(\sigma y_k^n + (1 - \sigma)y_{k+1}^n). \end{cases} \quad (8)$$

To record the finite-difference relations of the second time derivative on each spatial layer, the first-order accuracy relations are used, which are written in the grid nodes as  $(k, n)$  and  $(k + 1, n)$ . By setting the  $\sigma$  (8) parameter to a value of  $1/2$ , the second time derivative and the linear multiplier on the right-hand side of the nonlinear term can be agreed, also for the node  $(k + 1/2, n)$ . The combined explicitly/implicit difference Crank — Nicolson integration scheme (8) at each node of the finite-difference grid can be rewritten as (9), for the tridiagonal matrix algorithm:

$$\begin{cases} a_n x_k^{n-1} + b_n x_k^n + c_n x_k^{n+1} = d_n^x, \\ a_n y_k^{n-1} + b_n y_k^n + c_n y_k^{n+1} = d_n^y, \end{cases} \quad (9)$$

for  $k = \overline{1, K}$  and  $n = \overline{1, N}$ , where:

$$\begin{aligned}
a_n &= -\sigma, \quad b_n = 2\sigma - \frac{i\Delta t^2}{\Delta z} - 2\sigma(\theta\Phi_k^n + (1-\theta)\Phi_{k+1}^n), \quad c_n = -\sigma, \\
d_n^x &= (1-\sigma)(x_{k+1}^{n-1} - 2x_{k+1}^n + x_{k+1}^{n+1}) - \frac{i\Delta t^2}{\Delta z}x_{k+1}^n + (1-\sigma)(\theta\Phi_k^n + (1-\theta)\Phi_{k+1}^n)x_{k+1}^n, \\
d_n^y &= (1-\sigma)(y_{k+1}^{n-1} - 2y_{k+1}^n + y_{k+1}^{n+1}) - \frac{i\Delta t^2}{\Delta z}y_{k+1}^n + (1-\sigma)(\theta\Phi_k^n + (1-\theta)\Phi_{k+1}^n)y_{k+1}^n.
\end{aligned} \tag{10}$$

In order to match the recording of the nonlinear multiplier in (8) for the same node of the difference grid  $(k + 1/2, n)$ , it is also necessary to give the parameter  $\theta$  in (8) the value equal to  $1/2$ , which leads to the fact that system of equations (9) with respect to unknown quantities becomes nonlinear. To avoid such a problem helps the choice of the parameter  $\theta$  equal to zero. The simultaneous choice of parameters  $\sigma = 1/2$  and  $\theta = 0$  provides practical stability of the finite-difference scheme with the simultaneous possibility of reducing the system of equations at each integration step to a system of linear equations solved by the tridiagonal matrix algorithm [8].

The final system of equations takes the form (9) with the values of the tridiagonal matrix coefficients in the form (11):

$$\begin{aligned}
a_n &= -\sigma, \quad b_n = 2\sigma - \frac{i\Delta t^2}{\Delta z} - 2\sigma\Phi_{k+1}^n, \quad c_n = -\sigma, \\
d_n^x &= (1-\sigma)(x_{k+1}^{n-1} - 2x_{k+1}^n + x_{k+1}^{n+1}) - \frac{i\Delta t^2}{\Delta z}x_{k+1}^n + (1-\sigma)\Phi_{k+1}^n x_{k+1}^n, \\
d_n^y &= (1-\sigma)(y_{k+1}^{n-1} - 2y_{k+1}^n + y_{k+1}^{n+1}) - \frac{i\Delta t^2}{\Delta z}y_{k+1}^n + (1-\sigma)\Phi_{k+1}^n y_{k+1}^n.
\end{aligned} \tag{11}$$

For the coefficients at the edges, it is necessary to take into account the boundary conditions (7), and correct the coefficients  $b$ , which in general terms can be written as:

$$\begin{aligned}
db_1^x &= d_1^x - a_1 x_k^0, & db_{N-1}^x &= d_{N-1}^x - c_{N-1} x_k^N, \\
db_1^y &= d_1^y - a_1 y_k^0, & db_{N-1}^y &= d_{N-1}^y - c_{N-1} y_k^N.
\end{aligned} \tag{12}$$

For (9) and (11), the integration is carried out along the spatial coordinate, and the system of equations is solved on each spatial layer. Thus, the obtained difference scheme is a generalization of a special case of the Crank—Nicolson difference scheme, in which all linear terms of the equations are written according to an implicit finite-difference scheme, and the nonlinear term is taken from the previous computational layer. The integration is carried out in layers, from  $k + 1$  to the  $k$ -th layer along the  $z$  coordinate.

#### 4. Initial and boundary conditions

The initial conditions for solving the system of equations (9) with (11), (12) are the given values of the  $x$  and  $y$  arrays at  $k = K(z = -1)$  for all values of  $n = \overline{1, N}$ . In terms of the problem statement, the initial conditions (given values of the distribution of  $x$  and  $y$  as a function of time at the remote end of the optical fiber at  $z = 1$ ) determine the shape of the optical signal received at the remote end. Let's set, for example, at the remote end of reception of the ideal signal in the form of 16QAM with switching the information signal for  $x$  and for  $y$ . The system of equations (1), even if written in discrete-difference form (9) with (11), (12), requires that the desired functions  $x$  and  $y$  be continuous, along with their

second derivatives with respect to time and first derivatives with respect to space. Switching the information signal to 16QAM implies a discontinuity of both the function itself and its derivative. The use of a knowingly discontinuous function as initial conditions for solving the system of equations formulated for continuous functions immediately leads to unreliable results. In order to avoid the problem of breaking the initial data curves, the smooth joining technique of two discontinuous curves was used. The classical function that is conveniently used for these purposes is the hyperbolic tangent:

$$S(t, p, q) = \frac{1 - \text{th}(q(t - p))}{2}, \quad (13)$$

where  $t$  — an abscissa, along which it is necessary to sew two functions on the interval  $[t_0, t_N]$ ;  $p$  — a point from the interval  $[t_0, t_N]$ , determines the location of the joining;  $q$  — parameter responsible for the degree of smoothness of the joining.

For single switching information signal, the initial distribution and for the  $x$  and  $y$  represents the joining four functions in the interval  $[t_0, t_N]$ . The first interval is  $x(t) = 0$ ,  $y(t) = 0$  for  $t_0 < t \leq t_B$ ; the second segment is  $x(t) = 16\text{QAM}_{i_1}(t)$ ,  $y(t) = 16\text{QAM}_{j_1}(t)$  for  $t_B < t \leq t_M$ ; the third segment is  $x(t) = 16\text{QAM}_{i_2}(t)$ ,  $y(t) = 16\text{QAM}_{j_2}(t)$  for  $t_M < t \leq t_E$ ; the fourth segment is  $x(t) = 0$ ,  $y(t) = 0$  for  $t_E < t \leq t_N$ . The initial and final parts specified by zero values of  $x$  and  $y$  are determined by the requirements of the boundary conditions (7).

The initial distribution is given by discrete samples:

$$x_n = A_{\max} e^{-i\omega t_n} (S(t_n, p_M, q_M) \text{QAM}_{16}(i_B) + (1 - S(t_n, p_M, q_M)) \text{QAM}_{16}(i_E)) (1 - S(t_n, p_B, q_B)) S(t_n, p_E, q_E), \quad \text{for } n = \overline{1, N}. \quad (14)$$

In (14), the first multiplier forms the unmodulated carrier frequency, the second multiplier describes the switching at the  $p_M$  point of the 16QAM signal from the value determined by the  $i_B$  index to the value determined by the  $i_E$  index, with the smoothing parameter  $q_M$ . The third factor in (14) determines the switching of signals with zero boundary values at the points  $p_B$  and  $p_E$  with the corresponding smoothing parameters  $q_B$  and  $q_E$ .

Figure 2 shows the dependence of signal intensity  $x$  on time for its real part at the remote end of the fiber.

The imaginary part  $x$ , as well as the distribution for the real and imaginary parts of  $y$ , are not shown in the Fig. 2, because the imaginary and real parts of the signal are shifted relative to each other by a quarter of the period, and the distribution for  $y$  is similar. A fragment of the graph illustrating ensuring continuity when switching the 16QAM information signal is shown in the inset of Fig. 2. This shows that the smoothing technique provides both the continuity of the function itself and its derivative. In the places where switching from the information signal to the zero value, similar requirements of the continuity of the sought functions are provided together with their derivatives.

## 5. Ensuring the necessary accuracy of integration

Two layers along the spatial coordinate are the values of the sought functions on the  $k$  and  $k + 1$  layers for all values of  $n = \overline{1, N}$  over which integration is performed at each computational moment. Despite the absolute stability of the implicit Crank — Nicolson scheme, it is necessary to be sure that during the transition from layer to layer there is no loss of calculation accuracy and accumulation of error, which can become significant with

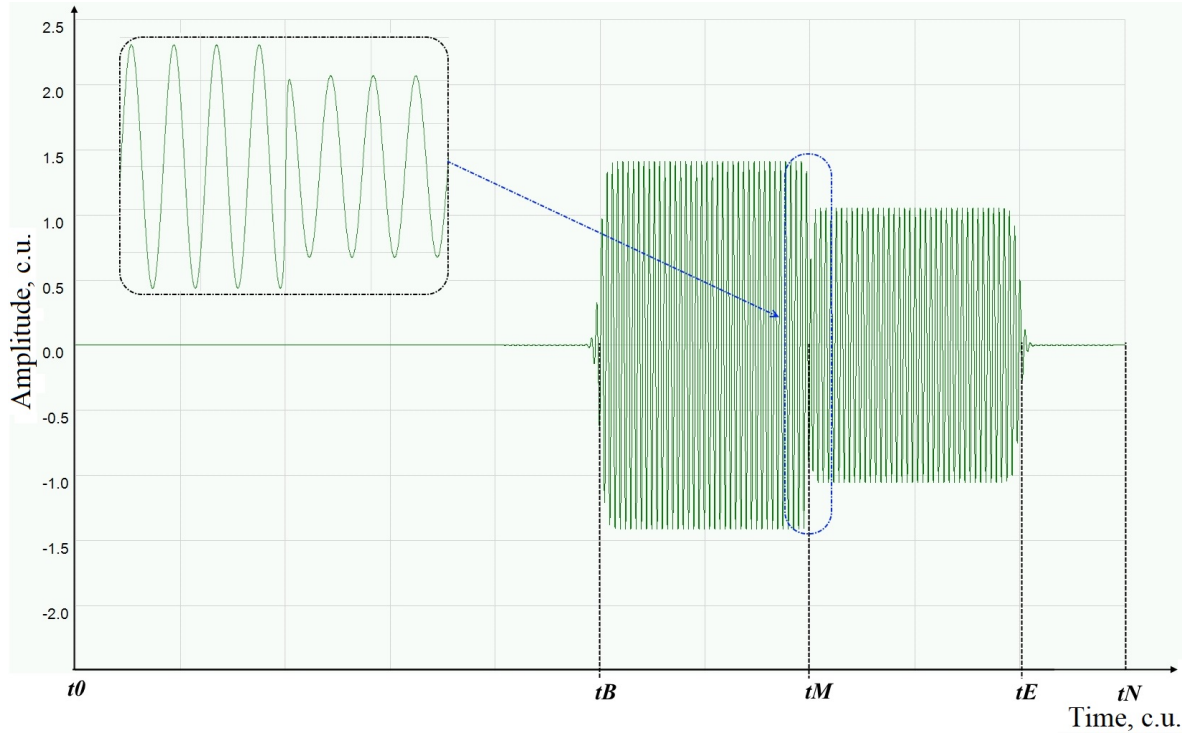


Fig. 2. The initial conditions for the real part  $x$  at the remote end of the optical fiber: the initial distribution and switching of the information signal from 0000 to 1001 in Gray standard coding

a sufficiently large number of integration steps along the spatial coordinate. In addition, it is necessary not to lose sight of the fact that the scheme proposed above does not use a purely implicit, but a mixed Crank — Nicolson scheme. There is an approach that helps to minimize the disadvantage that the nonlinear addend is used in the scheme in an explicit form.

The transition at each integration step from  $k$  to  $k + 1$  layers in space is carried out according to the following algorithm. The first step of the algorithm is to calculate the values of the sought functions  $x$  and  $y$  on the  $k$ -th unknown layer, using the values for the implicit multiplier (6) with  $k + 1$  of the calculated layer from the explicit scheme. Denote the calculated values of the functions on the  $k$ -th layer:

$$(x_k^n)_i \quad \text{and} \quad (y_k^n)_i, \quad (15)$$

for  $n = \overline{1, N}$  and  $i$  — an iteration number taken after the first run is a value equal to one.

Further, an iterative process is organized to find the desired functions  $x$  and  $y$  on the  $k$ -th unknown layer at the  $i + 1$  iteration. In this case, the implicit multiplier (6) in the computational scheme is corrected each time as if its value on the  $k$ -th layer is already known. The value on the  $k$ -th layer itself is taken as the half-sum of the values on the  $k$ -th and  $k + 1$  layers, but calculated at the previous iteration:

$$(\Phi_k^n)_{i+1} = \frac{(\Phi_k^n)_i + (\Phi_{k+1}^n)_i}{2}, \quad \text{for } n = \overline{1, N}, \quad (16)$$

The iteration process is carried out until the maximum difference between the values calculated on the  $i$  and  $i + 1$  iterations is less than the predetermined error:

$$\max(\max |(x_k^n)_{i+1} - (x_k^n)_i|, \max |(y_k^n)_{i+1} - (y_k^n)_i|) < \varepsilon, \quad \text{for } n = \overline{1, N}. \quad (17)$$

The proposed iterative process is rapidly converging and requires 3–7 iterations, depending on the specified error value.

## 6. Integration with variable step

Another factor that allows to increase the accuracy of calculations is the mechanism for automatic selection of the integration step. In this case, it is the automatic choice of the integration step by the spatial coordinate —  $\Delta z$ . The use of variable integration step allows to take into account the behavior of the solution and reduce the total number of steps, while maintaining the required accuracy of the approximate solution. Thus, the amount of work and machine time can be reduced and the growth of computational error is slowed down.

The algorithm for automatic selection of the integration step is traditional, where two sets of values of the sought functions are compared in the norm — the calculated two integration steps with a step  $\Delta z_j$ , and the calculated one integration step with a double step  $2\Delta z_j$ . In case the norm is lower than the specified error, the integration step is increased 1.1–1.3 times, and the current values are recorded. At the norm above the specified error, the integration step decreases by 0.7–0.9 times, and the integration steps are recalculated.

Combining integration with variable steps and an iterative process that levels the use of the explicit/implicit scheme gives quite good results.

## 7. Numerical results

To implement the proposed numerical method, a computer program was written in the C++ programming language. Figure 3 shows screenshots of the working area of the program, at all time points at different distances from the remote end of the optical fiber. In the left part of the program working area, the dependences of the sought functions  $x$  and  $y$  on time are displayed at different distances. On the upper right graph, the distribution of the perturbation of the function  $x$  (real — blue and imaginary — red parts) along the fiber from time at point 0.45 sr. units from the beginning of the fiber counted from the beginning of one. Service messages are displayed in the lower right part of the program, control buttons are located and calculation parameters are set.

Despite the fact that the discussion of the results of calculations is beyond the scope of the objectives of this article, below there are given some analysis results of this work. First, there is a noticeable influence of nonlinear distortions, which consist in a blurring of wave front and the distortion of the switching front of the information signal for 16QAM. Figure 3 shows a noticeable shift of the signal to the beginning of the time axis, with increasing distance from the far end of the optical fiber, which agrees well with the physical conditions for the propagation of optical disturbance in the fiber. The boundary conditions in the form of (2) (or (7)) determine that there was no disturbance in the entire fiber at the initial and final moments of time, in other words, there was a complete absence of a signal. However, the initial perturbation indicates that all perturbation is inside the fiber section. Therefore, the numerical calculation is possible only up to the moment when the signal was introduced into the optical fiber. Figure 3, *b* shows that with continued integration beyond the fiber section in which the perturbation is introduced, the perturbation is reflected from the beginning of time  $t = 0$ , which leads to results explained from a physical point of view.

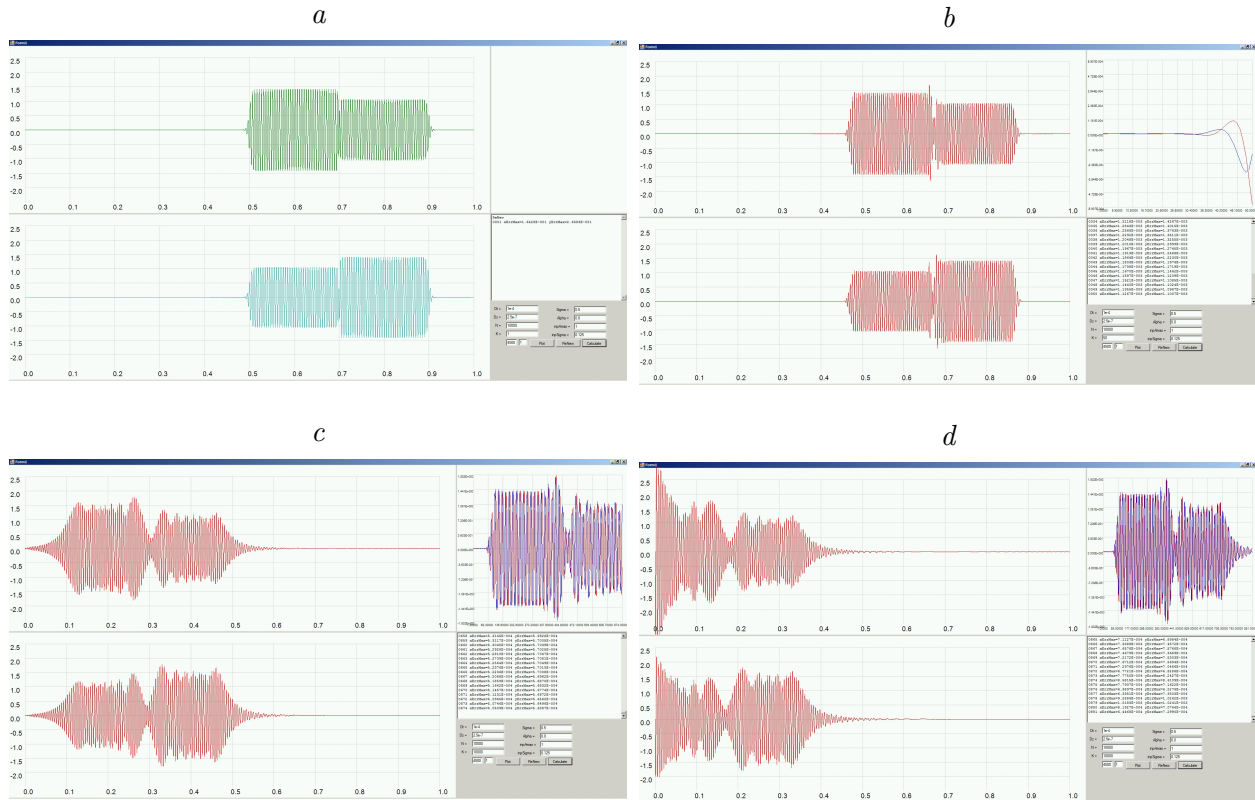


Fig. 3. The working screen of the numerical integration program of the equation system (5) for different values of the fiber length: *a* — at the fiber end (initial distribution); and at a distance: *b* —  $50 \times \Delta z$ ; *c* —  $674 \times \Delta z$ ; *d* —  $881 \times \Delta z$  from the remote end. Task parameters are:  $\Delta t = 10^{-4}$ ,  $\Delta z = 2.5^{-7}$ ,  $N = 10\,000$ ,  $\sigma = 0.5$

Figure 4 shows the calculations for the initial conditions, describing a single Gauss of a similar pulse in time, given only for the real part of the function  $x$ . The initial values of the imaginary part of the function  $x$  and the real and imaginary parts of the function  $y$  are set equal to zero.

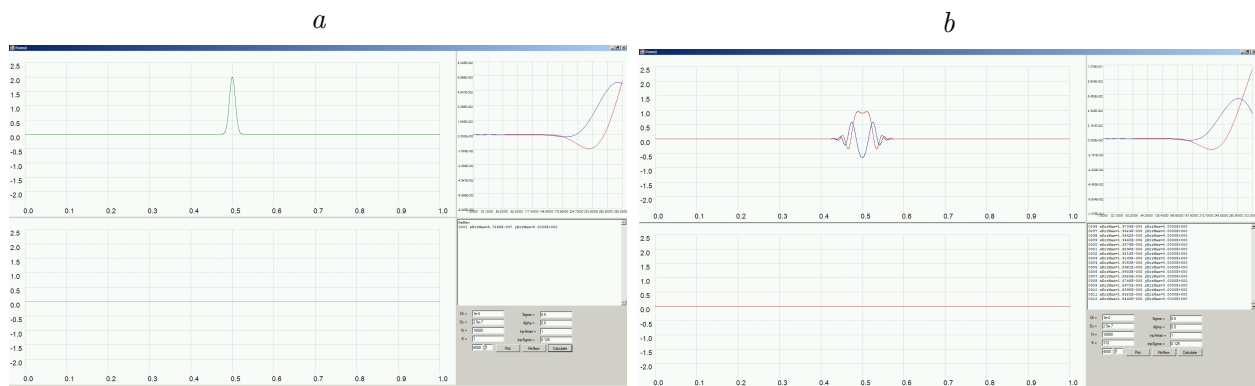


Fig. 4. The working screen of the program of numerical integration of the equation system (5) for the single Gauss of the similar pulse: *a* — at the end of the fiber (initial distribution); *b* — at a distance of  $312 \times \Delta z$  from the remote end of the fiber

The shape of the deformation signal of the similar Gaussian, the nature and form of the appearance of its imaginary part, corresponds to the results outlined in the works of other authors [9], which further indicates the correctness of the made assumptions, the chosen integration methods and the correctness of the obtained results.

## 8. Calculations for a long section of optical fiber

Distribution of the disturbance along the time axis from its current position to the beginning of the time reference point imposes a restriction on the possibility of calculations for extended sections of optical fiber. Combating this restriction directly leads to the need to dramatically increase the length of the arrays used to store information of the time interval containing all the disturbances from the beginning to the end, while ensuring that there is no disturbance in the entire fiber at the initial and final points of time.

However, there is an approach that can provide continuous integration for long sections of optical fiber. For this purpose, it is necessary to consider a time segment with a sliding integration window. Figure 5 shows an explanation diagram, which makes it possible to implement calculation algorithms for long sections of optical fiber without the need to increase the size of arrays.

The one-dimensional array that forms the sought functions on the  $k$ -th and  $k + 1$  spatial layers contains discrete samples with the values of the sought functions along the time axis. The initial distribution of the disturbance at the remote end looks like a dependence shown in the Fig. 5, bounded by a red frame (state A), and located in the array  $x$  from the first to the last ( $N$ ) element. With an increase of time  $t$  the disturbances shift relative to the array indices and at some point further integration will be difficult as the disturbance approaches the left border of the array — the blue frame in the Fig. 5 (state B). As soon as such a moment has arrived, it is sufficient to shift the perturbation curve with respect to the array, returning it to state A. With such a reindexing (displacement of the perturbation relative to the array indices), the values of the sought functions in the initial part of the array (in the Fig. 5 indicated by a blue dot-and-dash line) will be undefined. However, this disadvantage is easily remedied by smoothly stitching a part of the values in the array region that falls into both states (A and B) with the zero function. The values on the right-hand side (falling into state B, but not falling into state A) may be considered unnecessary.

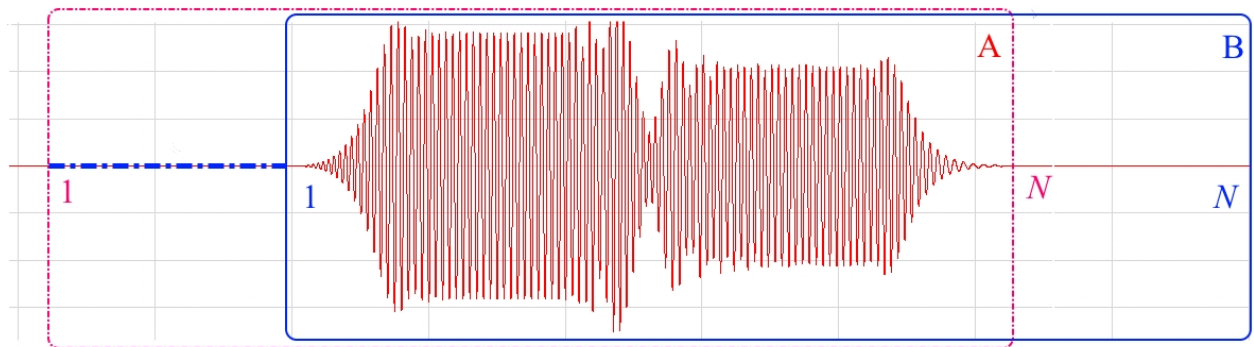


Fig. 5. Scheme explanation for the implementation of the calculation algorithms for long sections of optical fiber

## Conclusion

Finding an approximate solution of the Manakov equation system, associated with the modeling of optical communication lines based on multimode fibers, can be carried out using a combined explicit/implicit numerical integration scheme based on the Crank—Nicolson scheme. Writing an implicit term in the finite difference form, taken from the previous integration step, by itself gives a good result. An approach to the formation of the initial distribution 16QAM, which meets the requirements of continuity and smoothness of the sought functions, is proposed. The algorithm of automatic selection of the integration step ensures better convergence of the integration results over a long distance; moreover, it causes a decrease in the total number of integration steps. The proposed algorithm to refine the solution at each integration step allows levelling the deficiency of the proposed method for determining the implicit term from the previous integration step, which in turn allows integration to be carried out with larger step. Both of the proposed iterative algorithm for choosing the integration step and refining the solution at each step leads to a significant reduction in the total computation time and reduces the requirements for the size of the integration step. The algorithm has been tested that allows the calculation of compensation distribution parameters for extended fiber sections. The results of test calculations indicate the feasibility of the development of this algorithm in future.

**Acknowledgements.** The work was partly funded by the Ministry of Education and Science of the Russian Federation under the government project No. 8.6872.2017/8.9 of A.N. Tupolev Kazan National Research Technical University (KAI — Kazan Aviation Institute).

## References

- [1] **Burdin V.A., Volkov K.A., Bourdine A.V.** Approximate solution of coupled NLS equations. Proceedings of SPIE. Optical Technologies for Telecommunications. 2008; (7026):07–1–8. Available at: <https://doi.org/10.1117/12.801470>
- [2] **Andreev V.A., Burdin V.A., Bourdine A.V., Dashkov M.V.** Impact of mode coupling effects on few-mode optical fiber communication line performance. Proceedings of SPIE. Optical Technologies for Telecommunications. 2018; (10774):10774?19-01–10774-19-08. Available at: <https://doi.org/10.1117/12.2318888>
- [3] **Agrawal G.P.** Nonlinear fiber optics. 5th Edition. Boston: Academic Press; 2013: 648.
- [4] **Mumtaz S., Essiambre R.J., Agrawal G.P.** Nonlinear propagation in multimode and multicore fibers: Generalization of the Manakov equations. Journal of Lightwave Technology. 2013; 31(3):398–406. DOI:10.1109/JLT.2012.2231401
- [5] **Mecozzi A., Antonelli C., Shtaif M.** Coupled Manakov equations in multimode fibers with strongly coupled groups of modes. Optics Express. 2012; 20(21):23436–23441. DOI:10.1364/OE.20.023436
- [6] **Mecozzi A., Antonelli C., Shtaif M.** Nonlinear propagation in multi-mode fibers in the strong coupling regime. Optics Express. 2012; 20(11):11673–11678.
- [7] **Fedoruk M.P., Sidelnikov O.S.** Algorithms for numerical simulation of optical communication links based on multimode fiber. Computational Technologies. 2015; 20(5):105–119. (In Russ.)
- [8] **Sakhabutdinov Zh.M.** Analysis of discrete models of point motion. Kazan: Institute of Mechanics and Engineering; 1995: 196. (In Russ.)

- [9] **Ivanov D.V.** Metody i matematicheskie modeli issledovaniya rasprostraneniya v ionosfere slozhnykh dekametrovykh signalov i korrektsii ikh dispersionnykh iskazheniy [Methods and mathematical models for study of the propagation of decameter complex signals and correction its dispersion distortions]. Yoshkar-Ola: MarGTU; 2006: 266. (In Russ.)

---

Вычислительные технологии, 2020, том 25, № 2, с. 80–91. © ИВТ СО РАН, 2020  
Computational Technologies, 2020, vol. 25, no. 2, pp. 80–91. © ICT SB RAS, 2020

ISSN 1560-7534  
eISSN 2313-691X

---

ВЫЧИСЛИТЕЛЬНЫЕ ТЕХНОЛОГИИ

---

DOI:10.25743/ICT.2020.25.2.007

**Численные подходы к решению нелинейной системы уравнений Шрёдингера для распространения волн в оптическом волокне**

А. Ж. САХАБУТДИНОВ, В. И. АНФИНОГЕНТОВ, О. Г. МОРОЗОВ, Р. Р. ГУБАЙДУЛЛИН  
Казанский национальный исследовательский технический университет им. А.Н. Туполева — КАИ,  
Казань, Россия

Контактный автор: Сахабутдинов Айрат Ж., e-mail: azhsakhabutdinov@kai.ru

Поступила 4 сентября 2019 г., доработана 13 января 2020 г., принята в печать 30 января 2020 г.

**Аннотация**

Предложена разработка метода приближенного решения системы уравнения Манакова как одного из частных случаев системы уравнений Шрёдингера, связанного с моделированием оптических линий связи на основе многомодовых волокон. Решение ищется методами численного интегрирования. Показано, что численное интегрирование может быть осуществлено с использованием комбинированной явно-неявной схемы численного интегрирования на основе схемы Кранка — Николсон с записью нелинейного слагаемого в конечно-разностной форме, взятого с предыдущего шага интегрирования. Использован алгоритм автоматического выбора шага интегрирования, реализован итерационный алгоритм уточнения решения на каждом шаге, предложен алгоритм, позволяющий производить расчет параметров на протяженных участках. Нахождение приближенного решения системы уравнения Манакова может быть осуществлено с использованием комбинированной явно-неявной схемы Кранка — Николсон, а запись нелинейного слагаемого в конечно-разностной форме, взятого с предыдущего шага интегрирования, дает неплохой результат. Алгоритм автоматического выбора шага интегрирования обеспечивает лучшую сходимость результатов интегрирования на большом расстоянии и снижение необходимого количества шагов интегрирования. Алгоритм уточнения решения на каждом шаге позволяет нивелировать недостаток метода явной записи неявного слагаемого и интегрировать с большим шагом. Алгоритм расчета параметров распространения возмущения со сдвигом фрейма позволяет сделать вывод о целесообразности развития этого алгоритма.

*Ключевые слова:* Система уравнений Шрёдингера, система уравнений Манакова, явно/неявная схема Кранка — Николсон, распространение волн, распространение света в оптическом волокне.

*Цитирование:* Сахабутдинов А.Ж., Анфиногентов В.И., Морозов О.Г., Губайдуллин Р.Р. Численные подходы к решению нелинейной системы уравнений Шрёдингера для распространения волн в оптическом волокне. Вычислительные технологии. 2020; 25(2):80–91. (На англ. яз.)

**Благодарности.** Работа выполнена при финансовой поддержке Минобрнауки РФ в рамках государственного задания КНИТУ-КАИ № 8.6872.2017/8.9.